BIOCHEMISTRY
including biophysical chemistry & molecular biology

Article

pubs.acs.org/biochemistry

Myristoylation Exerts Direct and Allosteric Effects on Gα Conformation and Dynamics in Solution

Anita M. Preininger,[†] Ali I. Kaya,[†] James A. Gilbert, III,[†] Laura S. Busenlehner,[‡] Richard N. Armstrong,[†] and Heidi E. Hamm*,[†]

[†]Vanderbilt University Medical Center, Nashville, Tennessee 37232, United States

[‡]University of Alabama, Tuscaloosa, Alabama 35487, United States

Supporting Information

ABSTRACT: Coupling of heterotrimeric G proteins to activated G protein-coupled receptors results in nucleotide exchange on the Gα subunit, which in turn decreases its affinity for both Gβγ and activated receptors. N-Terminal myristoylation of Gα subunits aids in membrane localization of inactive G proteins. Despite the presence of the covalently attached myristoyl group, Gα proteins are highly soluble after GTP binding. This study investigated factors facilitating the solubility of the activated, myristoylated protein. In doing so, we also identified myristoylation-dependent differences in regions of Gα known to play important roles in interactions with receptors, effectors, and nucleotide binding. Amide hydrogen−deuterium exchange and site-directed fluorescence of activated proteins revealed a solvent-protected amino terminus that was enhanced by myristoylation. Furthermore, fluorescence quenching confirmed that the myristoylated amino terminus is in proximity to the Switch II region in the activated protein. Myristoylation also stabilized the interaction between the guanine ring and the base of the α5 helix that contacts the bound nucleotide. The allosteric effects of myristoylation on protein structure, function, and localization indicate that the myristoylated amino terminus of $G\alpha_i$ functions as a myristoyl switch, with implications for myristoylation in the stabilization of nucleotide binding and in the spatial regulation of G protein signaling.

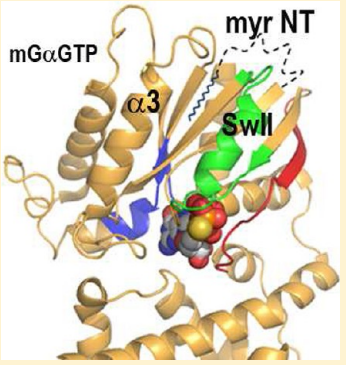

Heterotrimeric G proteins, consisting of α, β, and γ subunits, communicate extracellular stimuli to a variety of downstream effectors through seven-transmembrane G protein-coupled receptors. Receptors catalyze the release of GDP and binding of GTP to Gα subunits, which remain active until GTP hydrolysis and subsequent Gβγ association return the protein to the inactive, heterotrimeric state. While there are a multitude of G protein-coupled receptor subtypes, there are only a handful of G protein families that are responsible for communicating diverse inputs to a wide variety of effectors. How these many inputs and outputs are coupled through so few G proteins remains an open question in the field; however, it likely involves direct conformational as well as allosteric forces, further influenced by spatial and temporal mechanisms regulating G proteins and their binding partners in vivo. Examination of these influences in well-defined systems has allowed us to dissect individual contributions from moieties as small as the 14-carbon myristate, which is covalently bonded to the N-terminal glycine of all $G\alpha_i$ family members, including $G\alpha_t$, $G\alpha_z$, and $G\alpha_o$.

Crystal structures provide no information about the conformation of the myristoylated (myr) N terminus of activated Gα proteins. This is because no structure of a myrGα protein has been successfully determined, and structures obtained with unmyr proteins typically display disordered amino (N) termini in the absence of Gβγ;[1−13] thus, these structures shed little light on the conformation of the amino terminus in a myristoylated protein. Electron paramagnetic resonance (EPR) studies demonstrate the myr N terminus of GαGDP is ordered, even in the absence of Gβγ, in contrast to the more mobile N-terminal residues of unmyr Gα proteins.[14] The roles of co- and post-translational modifications of G proteins in membrane-delineated processes have been well documented in the literature,[15−22] but less is known about the structural and functional implications of myristoylation in activated $G\alpha_i$ subunits upon their release from activated receptors. Biophysical and biochemical studies such as this study provide unique insights into the conformation adopted by myrGα proteins in solution and, in particular, the orientation of the myr N terminus in the soluble, activated protein.

Our previous biochemical and biophysical studies suggest that, upon Gα activation, the myrN terminus participates in an intramolecular binding event on the surface of the Gα protein.[14,23,24] In this study, we used a combination of hydrogen−deuterium (H−D) exchange mass spectrometry (MS) and fluorescence studies. H−D exchange is ideally suited to evaluating solvent accessibility and protein dynamics. It is generally accepted that the extent of H−D exchange in the fast exchange regime reflects the solvent accessibility of the backbone, while the intermediate exchange regime is a consequence of conformational fluctuations of the protein. The time dependence of the exchange behavior is indicative of the conformational equilibria associated with

Received: September 20, 2011
Revised: February 10, 2012
Published: February 13, 2012

dynamics.[25−29] Using H−D exchange and fluorescence, we compared myr and unmyrGα_i proteins that had been activated with either AlF_4 or GTPγS. AlF_4 readily binds Gα_iGDP to form Gα_iGDP·AlF_4, which forms a mimic of the transition state present during GTP hydrolysis, and GTPγS activates Gα_i proteins more slowly as a result of basal nucleotide exchange of GDP for GTPγS on the Gα subunit. Guided by the H−D exchange experiments, we examined effects of myr on the environment of specific residues using fluorescence approaches. Fluorescence quenching studies were used to localize the position of the N terminus in the activated, myristoylated protein. Together, these biophysical approaches revealed direct and allosteric effects of myristoylation on the environment of residues throughout the activated protein. This solution study provides new insights into roles for myristoylation in the spatial regulation of G protein signaling.

MATERIALS AND METHODS

Materials. Porcine pepsin, GDP, and GTPγS were purchased from Sigma-Aldrich (Milwaukee, WI). Bodipy FL-GTPγS thioester and the cysteine-reactive probes monobromobimane and Alexa Fluor 594 C_5 maleimide were purchased from Invitrogen (Madison, WI). D_2O was purchased from Acros (Geel, Belgium). All other reagents and chemicals were of the highest available purity. ROS membranes containing rhodopsin and G$\beta_1\gamma_1$ were prepared as described in ref 30.

Protein Expression and Purification. Gα_i and Gα_i HI proteins containing an internal hexahistadine tag between residues Met[119] and Thr[120] of the Gα_{i1} sequence (*Rattus norvegicus*) were expressed and purified as described previously.[14,30,31] Construction, expression, and purification of Gα_i D328R were essentially as described in ref 32. Briefly, Gα_i proteins were expressed in *Escherichia coli*; for myr Gα_i, these were coexpressed with the pbb131 plasmid (courtesy of M. Linder) encoding *N*-myristoyltransferase and supplemented with myristic acid (30 μM). All proteins were then purified by Ni^{2+} affinity chromatography, followed by anion exchange high-performance liquid chromatography (HPLC) on a 5 mL Source Q anion exchange column (GE Healthcare, Piscataway, NJ). Chromatographic fractions were pooled on the basis of their ability to undergo activation-dependent changes in intrinsic Trp[211] fluorescence with a minimum of a 40% increase in fluorescence intensity upon activation[33] as seen in the intrinsic Trp fluorescence assay, or for proteins with mutation of residue 211, by BD-GTPγS binding.[34] Both labeled and unlabeled proteins were stored at −80 °C in 50 mM Tris, 100 mM NaCl, 2 mM $MgCl_2$, 1 mM DTT, 10 μM GDP, and 10% glycerol (pH 7.5).

Intrinsic Trp Fluorescence and AlF_4 Activation. Intrinsic tryptophan fluorescence was used to measure nucleotide exchange rates in Gα_i proteins, based on the ability of Trp[211] to act as a reporter of activation-dependent changes in solution.[33] Gα (200 nM) subunits are monitored by excitation at 280 nm and emission at 340 nm (ex/em 280/340 nm) before and after activation with 10 μM AlF_4 in 50 mM Tris, 100 mM NaCl, 2 mM $MgCl_2$, and 10 μM GDP (pH 7.5). Properly folded and functional Gα proteins exhibit a ≥40% increase in relative Trp fluorescence emission upon AlF_4 activation. The ability of selected Gα_i proteins to undergo activation-dependent changes as a result of basal nucleotide exchange of GDP for BD-GTPγS was measured as described previously,[32] with Gα_i HI proteins exhibiting a 10-fold higher rate of exchange than wild-type proteins because of the removal of solvent-exposed cysteines required for site-specific fluorescent labeling. Briefly, the emission intensity of Gα_i (200 nM) was monitored at ex/em 280/340 nm before and after addition of GTPγS (10 μM). Exchange of GDP for GTPγS results in enhanced Trp emission intensity, similar to the enhancement of the Trp emission intensity seen upon activation of Gα proteins with AlF_4. Intrinsic nucleotide exchange assays were performed in 50 mM Tris, 100 mM NaCl, and 1 mM $MgCl_2$ (pH 7.5) at 18 °C. All fluorescence experiments were conducted on a Varian Cary Eclipse instrument (Agilent, Santa Clara, CA). Changes in fluorescence emission were determined from a minimum of three independent experiments ± SEM. Time-dependent fluorescence changes were fit to an exponential association curve using Prism 4.0 (GraphPad Software). Mean values from at least three independent experiments that differ significantly are indicated: $*p < 0.05$, $**p < 0.01$, and $***p < 0.001$.

Peptide Identification and Hydrogen−Deuterium Exchange Analysis. To map peptides to the sequence of the protein, ESI MS/MS was performed essentially as described in ref 29. The extent of H−D exchange was measured by ESI LC−MS/MS[27] in the positive mode to detect charged ions. We probed the effects of myristoylation on solvent accessibility and protein dynamics by incubating the proteins in D_2O, which allows for exchange of backbone amide hydrogens with deuterium. The H−D exchange reaction was then quenched by decreasing the pH and temperature, and an acid-stable protease, pepsin, was used to cleave the protein. The increase in weight for each peptide, determined by MS analysis, revealed information regarding the solvent accessibility, conformation, and protein dynamics. The increase in weight of each peptide due to exchange of hydrogen for the 1 amu heavier deuterium over time was monitored, and fitting of the data across all data points revealed the rate and number of hydrogens being exchanged. Because side chain and N-terminal amide hydrogens are back exchanged during chromatography, exchange at these positions is not detected by this method.[27] Briefly, porcine pepsin was incubated with AlF_4-activated myrGα_i protein in a 1:1 (w/w) ratio in quench buffer containing 0.1 M KH_2PO_4 (pH 2.3) for a period of 5 min. Peptides were separated by reverse-phase HPLC on a microbore 1 mm × 50 mm Jupiter C18 column (Phenomenex) with a 2 to 98% acetonitrile gradient with 0.4% formic acid included in both mobile phases at 0.1 mL/min. Peptides were sequenced on a ThermoFinnigan TSQ Quantum (San Jose, CA) triple-quadrupole mass spectrometer in positive ion mode using data-dependent MS/MS collision-induced dissociation. Identities of the peptides were determined by using a combination of ESI MS/MS fragmentation, peptide mass searching of the Gα_i sequence using massXpert,[35] and predicted fragmentation patterns generated by MS-Product.[36] The amino acid sequences of the pepsin digests were determined by comparison of the MS/MS spectra to the predicted fragmentation patterns generated by MS-Product,[36] yielding approximately ≥85% sequence coverage (Figure 1A) by peptides that were sufficiently well-resolved to be used in the subsequent H−D exchange experiments.

The exchange of backbone amide hydrogens for deuterium in AlF_4-activated Gα_i proteins was initiated by addition of 5 μL of Gα_i protein (15 μg) to 45 μL of D_2O, and samples were incubated at 21 °C for time spans ranging from 15 s to 30 min. Following this incubation, reactions were quenched with 50 μL of quench buffer and mixtures immediately transferred to an ice bath and then allowed to digest with pepsin for an additional 5 min. The digested peptides were separated over 20 min with a 2 to 98% acetonitrile gradient containing 0.4% formic acid in all running buffers at a flow rate of 0.1 mL/min. In the LC−MS separation of deuterated peptides, the injection apparatus and

all chromatographic buffers were maintained at 0 °C by submersion in an ice/water slurry to minimize back exchange of deuterium during HPLC. To determine the extent of deuterium incorporation that occurred after quenching, a zero percent control ($m_{0\%}$) was prepared by addition of Gα_i to quench buffer at 0 °C, followed by addition of 45 μL of D_2O, and digestion with pepsin as described above. Furthermore, the amount of deuterium back-exchanged during chromatography was determined with a fully deuterated protein ($m_{100\%}$), which was obtained by incubation of Gα_i (15 μg) with 45 μL of D_2O at 45 °C for 8 h, followed by addition of quench buffer, and analyzed as described above. Data processing was performed using Finnigan Xcaliber (version 1.2). Peptide ions were located by mass searching, which resulted in a chromatographic ion profile for each ion that was averaged to obtain a composite spectrum for each ion. Magtran 1.0 beta 9[37] identified the centroid (m_t) of the given composite isotope envelope. The deuterium content of the peptides as a result of H−D exchange was corrected for gain ($m_{0\%}$) and loss ($m_{100\%}$) of deuterium during analysis according to eq 1

$$D = N\frac{m_t - m_{0\%}}{m_{100\%} - m_{0\%}} \quad (1)$$

where $m_{0\%}$, m_t, and $m_{100\%}$ are the average molecular masses for the same peptide in the undeuterated control, partially deuterated sample at time t, and fully deuterated control sample, respectively, and where N equals the total number of exchangeable peptide amide protons, minus one for the N terminus and any proline residues present. The amount of deuterium incorporated at each of nine different time points in each peptide was averaged in two independent experiments, with all data for one kinetic experiment collected on the same day, and plotted as a function of time. The time-dependent increase in mass as a result of H−D exchange was fit to single- or double-exponential equations as appropriate to the sum of first-order rate terms according to eq 2

$$D = N - \sum_{N}^{i=1} \exp(-k_i t) \quad (2)$$

where N is the number of amide hydrogens that exchange for deuterium at a given rate constant, k_i, during time t, the time point for which exchange was measured. Because of practical considerations in sample handling, the earliest time point measured was 15 s; therefore, hydrogens that exchange before this time point have an estimated k_i of >4 min^{-1}. Exchange is measured in two independent experiments for myr and unmyr proteins, at time points of 15, 30, 45, and 60 s and 2, 4, 10, 15, and 30 min. All time points were measured on the same day for a particular experiment. Average deuterium incorporation from two independent experiments was fit to an appropriate exponential equation using KaleidaGraph (Synergy Software, Reading, PA).

Protein Labeling. Gα_i HI proteins[31] were labeled with the indicated thiol-reactive probes. With a 5:1 probe:protein molar ratio and Gα_i HI proteins at a concentration of approximately 1 mg/mL in buffer free of reducing agent, proteins were labeled in 50 mM Tris, 130 mM NaCl, 2 mM $MgCl_2$, and 100 μM GDP (pH 7.5), followed by quenching with β-mercaptoethanol and removal of the unbound probe via HPLC using a SW2000 size exclusion column (Sigma-Aldrich, St. Louis, MO). The efficiency of labeling was between 25 and 40%, depending on the nature of the probe used, the location of the residue, and the time of labeling (generally 1−4 h). Chromatography was conducted in the same buffer supplemented with 10 μM GDP and 1 mM DTT. The monodispersity and molecular weight of the monomeric, labeled proteins used in this study after purification by gel filtration HPLC were confirmed through comparison of peak retention times and peak shape to results of a column calibration performed with a broad range of molecular weight standards run on the same day as the purified samples (Bio-Rad, Hercules, CA). The monomeric, labeled, purified proteins were pooled on the basis of their ability to undergo activation-dependent changes as measured by intrinsic Trp^{211} activation (described above). Proteins with Trp^{211} mutations were assayed by BD-GTPγS binding (described below) to ensure the functional integrity of the labeled proteins.

Extrinsic Fluorescence Assays. For bimane quenching experiments, emission of myr and unmyr Gα_i HI proteins (in complex with Gβγ, 150 nM each) specifically labeled at the third residue with monobromobimane (as described in Protein Labeling) was scanned between 400 and 600 nm, with excitation at 375 nm, before and after activation with 10 μM AlF_4 in 50 mM Tris, 100 nM NaCl, 2 mM $MgCl_2$, 10 μM GDP, and 1 mM DTT (pH 7.5). The time dependence of bimane quenching due to basal nucleotide exchange was based on the intrinsic basal nucleotide assay described in Intrinsic Trp Fluorescence and AlF4 Activation. Nucleotide exchange was initiated by addition of 10 μM GTPγS to bimane-labeled GDP-bound Gα HI proteins (200 nM) and fluorescence monitored at bimane-specific wavelengths (excitation and emission at 375 and 475 nm, respectively). For fluorescence studies of A1-labeled proteins, the emission maxima of 200 nM labeled Gα_i subunit were determined by scanning emission between 590 and 750 nm, with excitation at 580 nm. For BD-GTPγS binding,[34] the emission of BD-GTPγS (1 μM) was monitored at BD-specific wavelengths of 485 and 515 nm (excitation and emission, respectively) for 1 h after addition of Gα_i (200 nM), and for experiments with D328R protein, BD-GTPγS binding was measured with or without 10 μM AlF_4, in buffer consisting of 50 mM Tris, 100 mM NaCl, 2 mM $MgCl_2$, and 1 mM DTT (pH 7.5) at 18 °C. All fluorescence data were analyzed as described in Intrinsic Trp Fluorescence and AlF4 Activation.

Rhodopsin Binding Assay. The ability of labeled Gα_i subunits to bind rhodopsin in urea-washed ROS membranes was assessed as described previously.[32] Gα_i (5 μM) with Gβγ (10 μM) and rhodopsin (50 μM) in a buffer containing 50 mM Tris (pH 8.0), 100 mM NaCl, and 2 mM $MgCl_2$ were incubated in the dark, after light activation, and after light activation with the addition of GTPγS (100 μM) for 30 min at 4 °C. Membranes were separated by centrifugation at 20000*g* for 1 h, and the supernatants were removed from the pellets. For the dark fraction, the mixture was protected from light during centrifugation, and the supernatant was removed in dim red light. The isolated fractions were boiled, visualized via Coomassie-stained SDS−PAGE gels, and quantified by densitometry using a Bio-Rad Multimager by comparison of the amount of 37 kDa Gα in either pellet or supernatant to the total amount of Gα subunits in both fractions, expressed as a percent of the total. Data are averages of at least three independent experiments.

Tryptic Digest. Bimane-labeled myrGα_iHI W211F and unlabeled wild-type Gα_i protein (15 μM) in the GDP-bound and GDP·AlF_4-activated state were incubated with tosyl-phenylalanyl chloromethyl ketone trypsin at 4 °C in a 1:50 trypsin:Gα protein molar ratio. Samples were treated with tosyl-L-lysine chloromethyl ketone at a final concentration of 40 μg/mL for 5 min at 4 °C,

dx.doi.org/10.1021/bi201472c | *Biochemistry* 2012, 51, 1911−1924

prior to separation via SDS−PAGE and Coomassie staining (Figure S2B of the Supporting Information).[33]

RESULTS

Activation Results in a Highly Soluble myrGα Protein. We examined the effect of myr on membrane binding, before and after activation of the G protein by GTPγS. To do this, we measured the percent recovery of Gα protein in the pellet fraction versus that recovered in the soluble fraction in a reconstituted system consisting of rhodopsin in ROS membranes and Gα in complex with Gβγ. Like $G\alpha_t$, $G\alpha_i$ subunits bind Gβγ, and the reconstituted heterotrimer interacts with rhodopsin in an activation-dependent manner.[24,30,38] ROS membranes were prepared under dim red light, allowing examination of the membrane binding activity of G proteins in the dark, after receptor activation by light, and after addition of light and GTPγS. Densitometry of Coomassie-stained SDS−PAGE gels showed the relative amounts of Gα recovered in the pellet and supernatant fractions after incubation under the indicated conditions (Figure 1A,B),

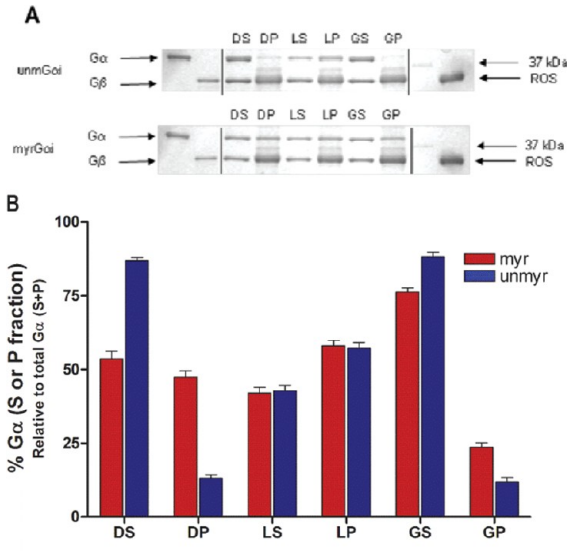

Figure 1. Myristoylation alters the protein localization and environment of residues in receptor-binding regions. (A) SDS−PAGE gels of indicated Gα proteins reconstituted with Gβγ prior to binding to ROS in the dark, in the light, and after light activation followed by addition of GTPγS, as described in Materials and Methods. Abbreviations: DS, supernatant from the dark sample; DP, pellet fraction in the dark; LS, light supernatant; LP, light pellet; GS, supernatant, with light and GTPγS; GP, pellet, with light and GTPγS. (B) Quantitation of data in panel A from densitometry of gels. Each bar (red, myr; blue, unmyr) is the average of three independent experiments; results are means ± SEM.

as described in Materials and Methods. Initially, myrGα is recovered to a greater extent in the membrane fraction than the unmyr (Figure 1A,B, lane DP, red vs blue) under dark conditions. Upon receptor activation, Gα proteins are equally well localized to the membrane (Figure 1A,B, LP lanes), and subsequent GTPγS binding releases activated subunits from membrane-bound receptors, facilitating recovery of both myr and unmyrGα in the supernatant (Figure 1A,B, GS lanes). Because myristoylation augments membrane association in the inactive, but not the active, state, we next sought to determine the factors facilitating the solubility of the activated protein.

Myristoylation Alters the Environment of the N Terminus and Other Regions throughout the Activated Protein. To investigate the activation-dependent solubility of myrGα, we performed H−D exchange analysis. In particular, we were interested in the ability of amide hydrogens in the myr N terminus to exchange with deuterium, as a means of investigating the solvent exposure and conformational flexibility of this region. Intact, AlF_4-activated $G\alpha_i$ (myr and unmyr) was exposed to D_2O for varying periods of time, followed by quenching and enzymatic cleavage as described in Materials and Methods. Subsequent MS analysis of the products allowed direct measurement of the number of backbone amide hydrogens that exchange with deuterium during the assay.[27] After mapping the individual peptides to the primary sequence (Figure S1 of the Supporting Information) using high-resolution LC−MS/MS, we measured the time dependence of H−D exchange in peptides that were well-resolved in both myr- and unmyr$G\alpha_i$ proteins. The nine time points tested for each protein ranged from 15 s to 30 min. The average H−D exchange at each time point was then fit to an appropriate exponential equation. The *y*-intercept of the fitted line provides an estimate of the number of backbone amide hydrogens that exchange in the first 15 s. The percentage of hydrogens in each peptide that exchange in this fast exchange regime is shown in Figure 2, which reflects the solvent (D_2O) accessibility of the specific region of the protein.[25] The kinetic plots also reveal the number and rates of backbone hydrogens that exchange over the entire time course of the experiment. These data, along with statistics for evaluating the quality of the data fitting, are listed in Table S1 of the Supporting Information. From this analysis, we observed qualitative similarities between myr and unmyr proteins, consistent with their ability to bind Gβγ, nucleotides, and receptors and hydrolyze GTP, with subtle myr-dependent differences in regions throughout the Gα protein.

A Number of Regions Display Relatively Similar Fast H−D Exchange, Regardless of Myristoylation. In comparing the percentage of fast-exchanging hydrogens in the activated myr and unmyr proteins, we observed a qualitatively similar trend across the primary sequence regardless of myristoylation (Figure 2A) in some regions of the Gα proteins. For example, in both myr and unmyr proteins, regions that displayed the highest percentage of fast exchange included the peptide that encompassed the hexahistadine tag (denoted with an asterisk), followed by the extreme C terminus (residues 341−353), the αA/αB loop (residues 92−103), and a peptide spanning the C-terminal end of the α2 helix and the α2/β4 loop (residues 209−222), with ≥50% of the amide hydrogens exchanging before the first time point in both myr and unmyr proteins (Figure 1B, top gray dashed line). Regions with a relatively low percentage of fast-exchanging protons regardless of myristoylation included residues 9−18 and 24−34 in the N terminus, residues 37−52 containing the phosphate binding loop (P-loop), and portions of the αC, αD, and αE helices, residues 124−139, 140−153, and 154−159, respectively, with ≤30% of the amide hydrogens undergoing fast exchange (Figure 1B, bottom gray dashed line). The β3/α2 region (residues 196−208), α3 helix (residues 241−249) and residues preceding it (residues 232−234), β5 strand (residues 267−274), β6/α5 loop (residues 322−330), and several residues in the C-terminal α5 helix (residues 334−336) also exhibit a low percentage of amide hydrogens undergoing fast exchange regardless of myr. These results reveal information about the accessibility of the backbone amide hydrogens to D_2O, relevant to the conformation the protein adopts in solution. These results also revealed subtle effects of myristoylation on various regions throughout the Gα protein.

dx.doi.org/10.1021/bi201472c | *Biochemistry* 2012, 51, 1911−1924

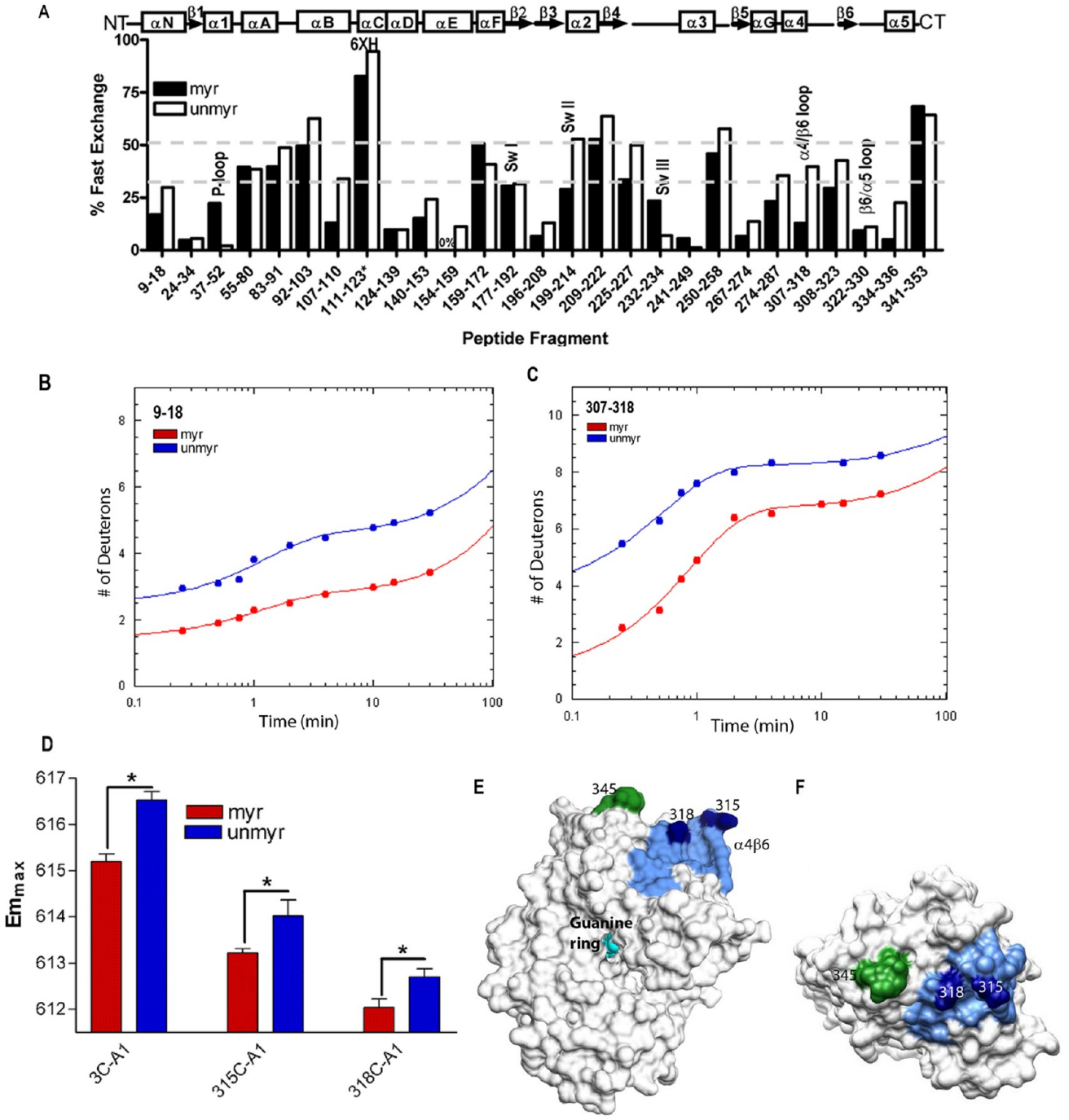

Figure 2. (A) Myristoylation allosterically modifies the environment of multiple regions within the activated Gα protein. Shown is the percentage of deuterium incorporation in each peptide as a percent of the total number of exchangeable backbone amide hydrogen in each peptide (y-axis), which occurs as a result of fast H−D exchange in the indicated peptides of myrGα_i (filled bars) and unmyrGα_i (empty bars), shown on the x-axis. The fits for all peptides can be found in Table S1 of the Supporting Information and the peptide cleavage map of the protein in Figure S1 of the Supporting Information. Regions of secondary structure are indicated along the top. The label 111−123* denotes the peptide that encompasses the hexahistadine tag (unnumbered) located between residues 119 and 120. Gray dotted lines indicate peptides with an overall high (≥50%, top dashed gray line) or low (≤30%, bottom dashed gray line) solvent accessibility regardless of myristoylation. (B and C) H−D exchange kinetic rate profiles for peptides encompassing residues 9−18 (B) and 307−318 (C). Shown are the time dependencies of incorporation of deuterium into peptides originating from myrGα_iGDP·AlF_4 (red spheres) and unmyrGα_iGDP·AlF_4 (blue spheres) as a function of incubation time in D_2O. Each time point is the average of two independent experiments; results were fit to a single- or double-exponential equation according to eq 2, with fitted parameters listed in Table S1 of the Supporting Information. (D) em_{max} for the indicated A1-labeled Gα_i HI proteins after AlF_4 activation was determined as described in Materials and Methods from excitation at 580 nm and scanning peak emission between 590 and 750 nm in a minimum of three independent experiments; results are means ± SEM. (E and F) Surface of unmyrGα_iGDP·AlF_4, from PDB entry 1GFI,[2] with the last resolved residue in the C terminus colored dark green, shown to indicate the receptor-binding face of the protein. Light blue indicates the $\alpha4/\beta6$ loop region, with darker blue indicating the position of indicated $\alpha4/\beta6$ residues that were analyzed in panel D: (E) side view and (F) view of the protein that faces the receptor. The surface of 1GFI[2] was rendered with Chimera.[66]

dx.doi.org/10.1021/bi201472c | *Biochemistry* 2012, 51, 1911−1924

Regions throughout the Gα Protein Display myr-Dependent Alterations in Fast H−D Exchange. While general trends in fast exchange across the protein were qualitatively similar, a number of regions displayed myr-dependent differences in the percentage of fast-exchanging hydrogens. The myrN-terminal peptide displayed a >10% reduction in fast exchange due to myristoylation (Figure 2A). Surprisingly, several regions far removed in sequence from the N-terminal myristoylation site also displayed a >10% reduction in fast exchange due to myristoylation. These regions included residues in the αB region (residues 107−110), αE (residues 154−159), Switch II (SwII, residues 199−214), residues in the β4 strand (residues 225−227), α3 helix (residues 250−258), residues within the αG helix (residues 274−287), the α4/β6 loop (residues 307−318), and nearby residues 308−323, as well several residues in the α5 helix (residues 334−336). While myristoylation generally conferred reductions in the percentage of fast-exchanging hydrogens, there were several regions that showed myr-dependent enhancements (>10%) in fast exchange, including the peptide that encompasses the P-loop (residues 37−52), as well as a small segment of Switch III (SwIII, residues 232−234). Because the myr proteins are highly membrane localized, we next sought to determine how the environment of receptor-binding regions in the activated state might support a cytosolic localization for the myr protein.

Myr-Dependent Differences between the N Terminus and α4/β6 Loop. Several of the regions that displayed myr-dependent differences in H−D analysis are located in regions known to be involved in receptor binding, and because of the critical role of these regions, we selected them for further study. We noted myr-dependent differences in the percentage of fast-exchanging hydrogens in the N terminus and the α4/β6 loop,[24,39,40] as indicated by differences in the *y*-intercepts of the fitted lines in panels B and C of Figure 2. To investigate this further, we next used site-directed fluorescent labeling to examine the environment of specific residues within each of these regions, to examine myr-dependent differences at the residue level. We introduced cysteines at sites of interest in the background of a cysteine-depleted parent $G\alpha_i$ HI protein.[31] We labeled residues in the N terminus and the α4/β6 loop of three separate $G\alpha_i$ HI Cys mutants with a thiol-reactive Alexa^{595} (A1) probe. The A1 probe has been shown to exhibit a lower em_{max} (blue shift) of ∼10 nm in hydrophobic environments as compared to its em_{max} in more polar environments.[24] Individually labeled myr and unmyr$G\alpha_i$ HI 3C-A1, 315C-A1, and 318C-A1 were activated with AlF_4 as described in Materials and Methods, and the em_{max} values of the myr and unmyr proteins were compared (Figure 2D). Because the first well-resolved peptide in common to both myr and unmyr proteins started with residue 9 in the H−D exchange analysis, the ability to specifically label residue 3 provided a measure of the environment closer to the extreme N terminus. We observed a statistically significant myr-dependent blue shift in the em_{max} values of all three proteins, consistent with myr-dependent decreases in polarity surrounding these labeled residues in the activated proteins. The α4/β6 loop (Figure 2E,F, light blue) and residues 315 and 318 (Figure 2E,F, dark blue) in this region are visible in crystal structures of activated, unmyr$G\alpha_i$,[2] near the last resolved residues in the C terminus, colored green in panels E and F of Figure 2 for reference. Because similar fluorescence studies conducted with specifically labeled residues in the C terminus failed to detect any myr-dependent decreases in em_{max} (not shown), this indicates that the myr-dependent blue shifts we detected in fluorescently labeled residues in the α4/β6 loop region are not likely due to interactions with nearby C-terminal residues, which exhibit a high level of fast exchange regardless of myristoylation (Figure 2A). In addition to receptor-binding regions, regions known to be involved in binding nucleotide also exhibited myr-dependent differences in fast exchange.

Myr-Dependent Differences in Regions That Interact with the Guanine Ring. Interestingly, H−D exchange revealed unexpected myr-dependent differences in fast exchange in regions with well-established roles in nucleotide binding, such as the base of the α5 helix, which interacts with the guanine ring. To examine the effect of myr on nucleotide binding, we used an extrinsically labeled GTP analogue, Bodipy-GTPγS (BD-GTPγS) (Figure 3A, inset), as a reporter of environmental differences surrounding the bound nucleotide. While it is known that BD-labeled nucleotides bind Gα subunits with a lower affinity than unlabeled nucleotides, we can compare the relative ability of myr and unmyr proteins to bind to this GTP analogue. Because BD-GTPγS binds Gα subunits with a lower affinity than unlabeled GTPγS,[32,41] we competed away bound BD-GTPγS with a 10-fold excess of unlabeled GTPγS. The time dependence of the decrease in BD-GTPγS emission (Figure 3A) upon addition of unlabeled GTPγS was significantly slower in the myr protein than in the unmyr protein (Figure 3A, solid line vs dotted line, **p*, 0.002 ± 0.0009 vs 0.004 ± 0.0001 s^{-1}, respectively), revealing a myr-dependent enhancement in BD-GTPγS binding.

Activation with AlF_4 Offsets the Destabilizing D328R Mutation in the Myristoylated Gα Protein. To determine if the myr-dependent enhancement of BD-GTPγS binding was due to allosteric effects of myr on regions involved in binding the guanine ring, we examined H−D exchange in regions surrounding the guanine ring. We noted that, of the two peptides flanking the guanine ring (Figure 3B), only peptide 322−330 exhibited a myr-dependent reduction in the time dependence of H−D exchange (panels C and D of Figure 3, respectively). This peptide encompasses residue 328; mutation of this residue (and others around it) is known to markedly elevate the level of nucleotide exchange.[32,41] However, it is known that, in wild-type $G\alpha_i$ proteins, addition of AlF_4 severely reduces the level of exchange of GDP for GTPγS, using either unlabeled GTPγS[2] or BD-GTPγS.[32] This indicates AlF_4 binding can stabilize bound GDP, regardless of the nucleotide analogue used in the exchange assay. However, unlike wild-type $G\alpha_i$, even addition of AlF_4 does little to prevent exchange of GDP for BD-GTPγS in the unmyr$G\alpha_i$ D328R protein.[32] Because myr reduced the time dependence of H−D exchange in the region encompassing residue 328, we reasoned that myr may stabilize the D328R protein against exchange. Because the maximal level of fluorescence after GDP−GTPγS exchange differs for myr and unmyr proteins (see below), we set the maximal fluorescence for each protein to 1.0. We then measured the effect of addition of AlF_4 on nucleotide exchange in the myr D328R protein, as compared to unmyr, as described in Materials and Methods. We found that myristoylation significantly enhanced the AlF_4-mediated stabilization of bound GDP, weakening overall BD-GTPγS binding (Figure 3E, right two bars). This indicates that myr stabilizes interactions between the base of the α5 helix and the guanine ring that is specifically perturbed by the D328R mutation located within this region (Figure 3B). We next examined interactions between the nucleotide and the phosphate binding corridor, which accommodates binding to GDP, GTP, and GTP analogues with substitutions in and around the β- and γ-phosphates.

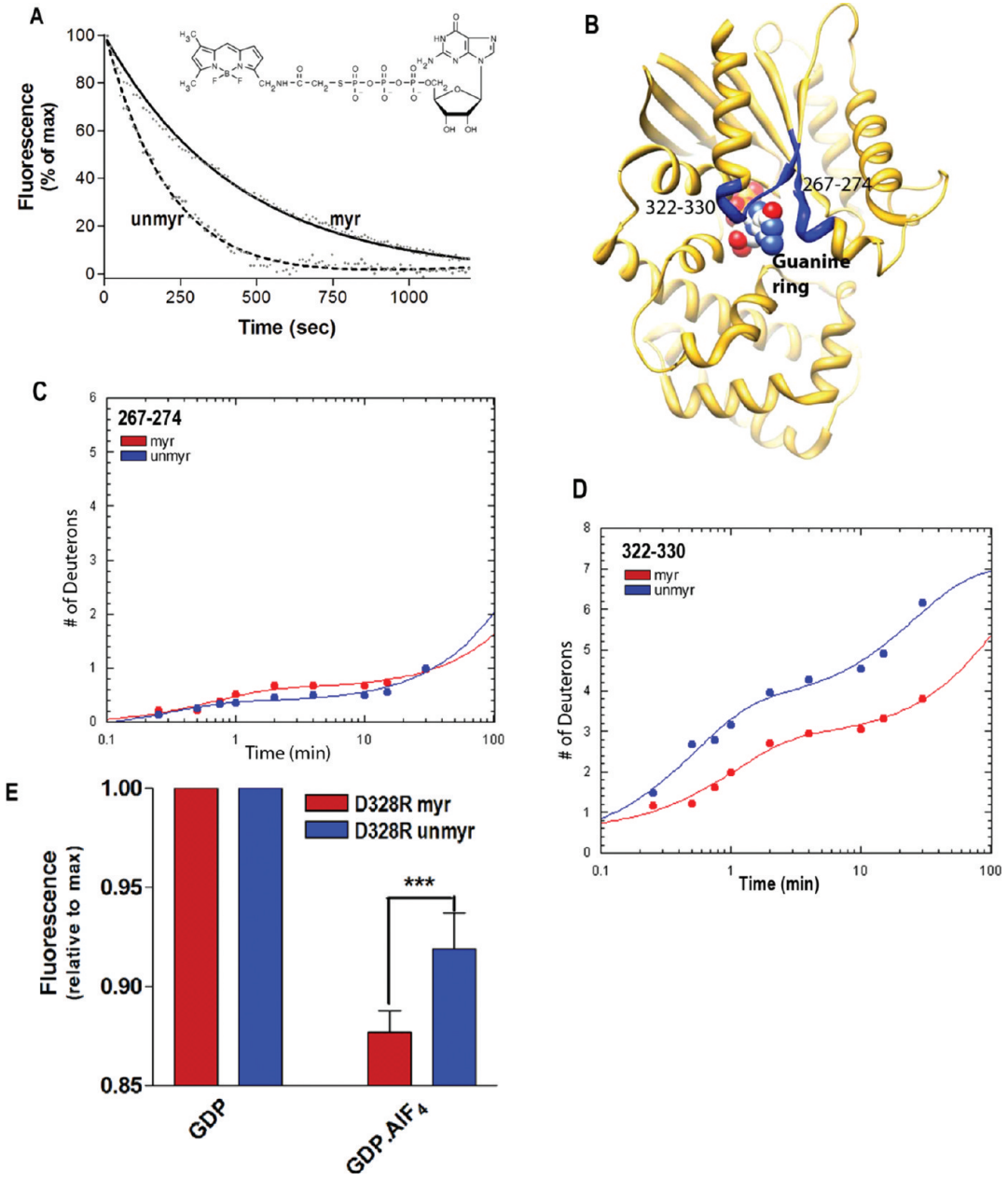

Figure 3. Protein−nucleotide binding interactions influenced by myristoylation. (A) $G\alpha_i$GDP proteins were preloaded with 1 μM BD-GTPγS for 1 h, and dissociation was initiated at time zero by addition of 10 μM unlabeled GTPγS [emission monitored with excitation and emission wavelengths of 485 and 515 nm, respectively (ex/em 485/515 nm)] as described in Materials and Methods. Data points are the average of three independent experiments, which were fit to a single-exponential dissociation curve using GraphPad Prism 4.0. The inset shows the structure of BD-GTPγS used in these studies (Invitrogen, Madison, WI). (B) Regions of $G\alpha_i$ that surround the guanine ring (PDB entry 1GFI,[2] rendered with Chimera[66]) are shown as blue ribbons. (C and D) Time dependence of H−D exchange (as described in the legend of Figure 2) for (C) peptide 267−274 flanking the guanine ring and (D) peptide 322−330 located at the base of the α5 helix. (E) Myr-dependent stabilization of interactions between the guanine ring and residue 328 located at the base of the C-terminal α5 helix. The left two bars show the maximal level of BD-GTPγS fluorescence (ex/em 485/515 nm) for each protein exhibited upon full BD-GTPγS binding measured after 1 h (set to 1.0). The right two bars show preactivation of GDP-bound proteins with 10 μM AlF_4 for 5 min prior to addition of BD-GTPγS reduces the extent of exchange of GDP·AlF_4 for BD-GTPγS, as compared to their respective maxima. Data are averages of three independent experiments; results are means ± SEM.

Myristoylation Enhances the Polarity of the Phosphate Binding Corridor. On the opposite side of the nucleotide binding pocket, residues important for hydrolysis of the γ-phosphate of GTP line the phosphate binding corridor. To examine effects of myr on the phosphate binding corridor, we took advantage of another unique characteristic of BD-GTPγS: it has the fluorescent moiety linked to the terminal phosphate (Figure 3A, inset). This provides a convenient sensor of interactions between residues in the phosphate binding corridor and bound nucleotide in the vicinity of the third phosphate. While myr and unmyr$G\alpha_i$ proteins exhibited similar rates of BD-GTPγS binding (0.001 ± 0.0001 s^{-1}), myristoylation resulted in a consistently lower overall maximal emission intensity of the probe after full exchange had occurred (Figure 4A), an effect seen in both wild-type and mutant $G\alpha_i$ proteins. The lower maximal fluorescence for myr$G\alpha_i$ upon

dx.doi.org/10.1021/bi201472c | *Biochemistry* 2012, 51, 1911−1924

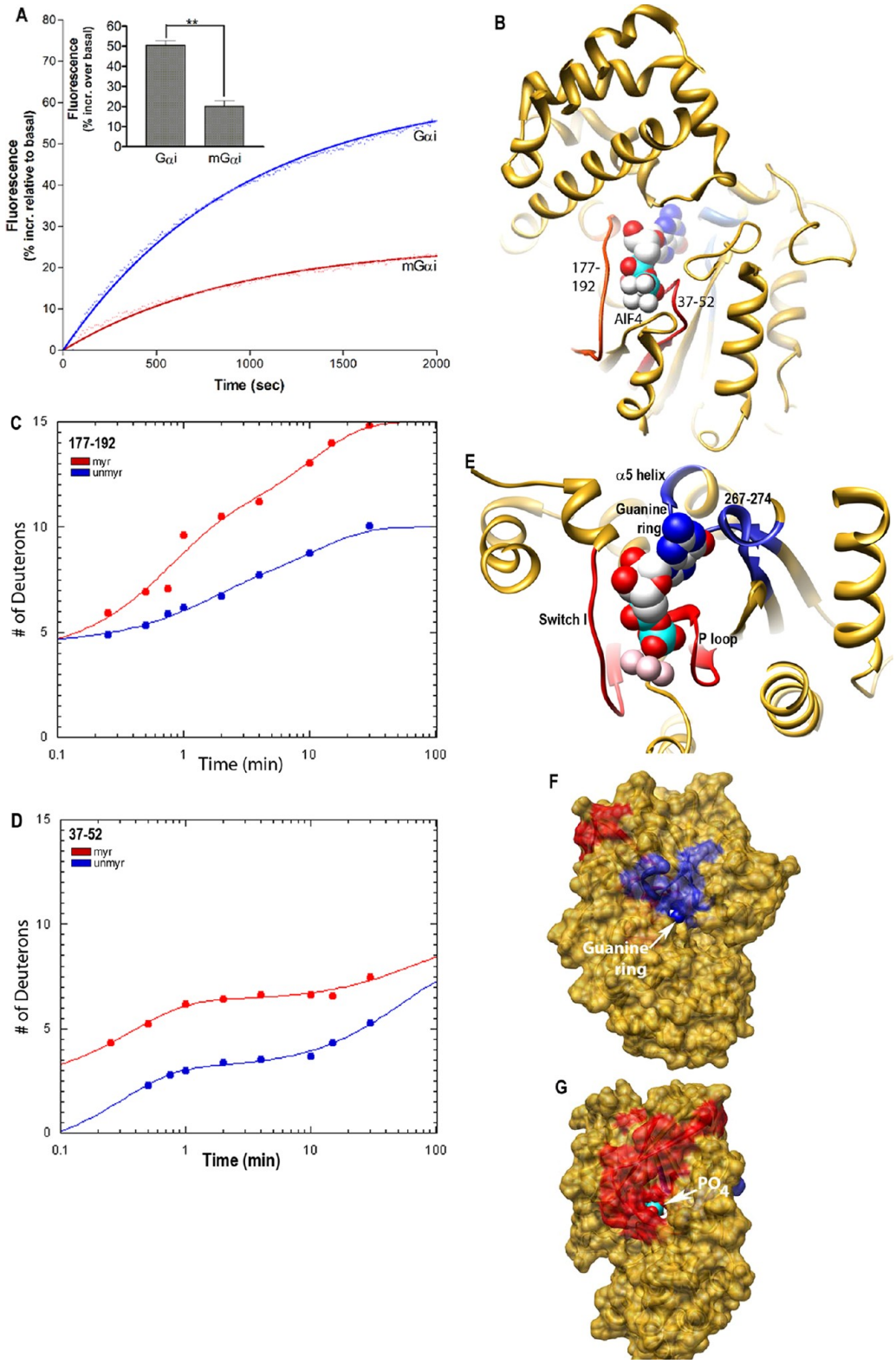

Figure 4. Gα–nucleotide interactions along the phosphate binding corridor. (A) Representative trace of BD-GTPγS fluorescence increases (ex/em 485/515 nm) upon binding to myrGα_i (red) and unmyrGα_i (blue), shown relative to basal BD-GTPγS fluorescence prior to addition of Gα and fit to a single-exponential association curve using GraphPad Prism 4.0 as described in Materials and Methods. The inset shows the quantitation of the maximal increase using data from three independent experiments ± SEM. (B) Red denotes regions in the phosphate binding corridor (PDB entry 1GFI,[2] rendered with Chimera[66]), which were analyzed by H–D exchange. (C and D) Time dependence of H–D exchange (as described in the legend of Figure 2) for peptides in SwI, residues 177–192 (C), and the P-loop, residues 37–52 (D), both highlighted in red in panel B. (E) Ribbon view of interactions surrounding the bound nucleotide in activated Gα_i proteins (PDB entry 1GFI,[2] rendered with Chimera[66]), colored as in Figure 3B and panel B of this figure. Regions of high solvent accessibility and/or protein dynamics in the phosphate binding corridor are colored red, and regions with reduced protein dynamics and/or solvent accessibility surrounding the guanine ring are colored blue. (F and G) Chimera surface rendering of panel E, with B and C rotated approximately 180° about the vertical axis.

dx.doi.org/10.1021/bi201472c | *Biochemistry* 2012, 51, 1911–1924

binding to BD-GTPγS indicates there is a more polar environment surrounding the labeled nucleotide near the region of the third phosphate due to myristoylation.

Regions that contribute residues important for nucleotide binding and hydrolysis include the SwI region and P-loop,[2,3] encompassed by peptides 177−192 and 37−52, respectively (Figure 4B, colored red). Although the percentage of hydrogens undergoing fast exchange in the region encompassing SwI residues 177−192 is similar regardless of myristoylation, this region nevertheless exhibited a myr-dependent increase in the dynamics of H−D exchange (Figure 4C). Furthermore, there was an increase in the fast H−D exchange for residues 37−52 in the P-loop region of the myr protein (Figure 4D). This myr-dependent increase in the percentage of fast exchange in the P-loop is also consistent with a more polar environment surrounding the Bodipy group linked to the third phosphate of GTPγS that we detected in the myrGα_i protein (Figure 4A). Depictions of regions surrounding the guanine ring and in the phosphate binding corridor described above are shown as ribbons (Figure 4E) and space-filled views (Figure 4F,G) for reference. These results indicate that regions involved in nucleotide binding are altered by myristoylation, including regions surrounding the guanine ring and those lining the phosphate binding corridor.

Myristoylation Alters the Environment of Residues in the SwII Region. Given the effects of N-terminal myristoylation on regions involved in nucleotide binding and hydrolysis, we next examined the effect of myristoylation on interactions with the SwII region. This Switch region is known for its ability to report activation-dependent changes in conformation through changes in the emission of Trp^{211} located in this region, which exhibits enhanced emission because of the decrease in the polarity of its environment upon activation.[42] While the time dependence of H−D exchange in SwII was unaltered by myristoylation, there was a myr-dependent decrease in the number of hydrogens undergoing fast H−D exchange, that is, exchange that occurs prior to the first time point of 15 s (Figure 5A). To examine the environment of specific SwII residues, we compared the em_{max} of AlF_4-activated myr and unmyrGα_i HI proteins labeled at residues 209 and 211 (Figure 5B). Both of the labeled proteins retained the ability to undergo activation-dependent changes as described in Materials and Methods. Residue 211 reported a significant myr-dependent blue shift in em_{max}, consistent with a more hydrophobic environment for this residue in the myr protein, unlike effects on nearby residue 209. Because SwII residues do not directly contact bound nucleotide, and because a previous study demonstrates that myristoylation influences the environment of the SwII Trp,[23] we next investigated the interaction between the myr N terminus and the SwII region.

Localization of the myr N Terminus in the Activated Gα Protein. To determine if the reductions in solvent accessibility and exposure in the N terminus and SwII were due to a direct binding event between these regions, as suggested previously,[23] we performed bimane quenching experiments. Bimane quenching relies on the ability of tryptophan to quench bimane fluorescence when the fluorophore is within 15 Å of a tryptophan residue.[43] The following experiments, designed to localize the N terminus, were confined to myr proteins; because all Gα_i proteins are permanently myristoylated, interactions of the unmyrN terminus are of little relevance to signaling in vivo. We labeled the myr N terminus of 3C-Gα_i HI at the third residue with a thiol-reactive bimane probe and scanned the protein's emission at bimane-specific wavelengths before and after activation of the protein with AlF_4 (Figure 5C). The activation-dependent quenching evidenced by decreased emission from the probe upon activation indicated that the third residue closely approached one or more Trp residues in Gα_i. Because there are two Trp residues in the GTPase domain, Trp^{258} and Trp^{211}, near the last resolved residues in the N terminus of Gα_iGDP·AlF_4 (Figure 5D, Trp side chains colored green, N terminus colored red), we individually mutated each of these to Phe. We then repeated the quenching experiment as described in Materials and Methods; only mutation of Trp^{211} was able to significantly relieve the activation-dependent quenching (Figure 5E, center bar) of the N-terminal bimane probe, unlike nearby Trp^{258}. All of the proteins are competent to undergo activation-dependent conformational changes in a manner similar to that of the wild-type protein, as measured by the >40% increase in the intrinsic Trp fluorescence for proteins containing a native Trp residue at position 211, as described in Materials and Methods. Because mutation of residue 211 precludes the use of the Trp activation assay, the ability of the bimane-labeled Trp^{211} mutant was assayed by BD-GTPγS binding and tryptic digests. These controls demonstrate that the protein binds GTP analogues, and that the labeled protein can undergo AlF_4-mediated activation in a manner similar to that of the wild-type protein, which protects it from tryptic digestion (Figure S2A,B of the Supporting Information).

To investigate the relevance of the activation-dependent quenching of bimane fluorescence to conformational changes in SwII that occur upon activation, we compared the time dependence of the quenching to the time dependence of Trp fluorescence, both upon exchange of GDP for GTPγS. We chose this measure because uncatalyzed GDP−GTPγS exchange in Gα proteins occurs at rates that are specific for each Gα isoform, and Trp fluorescence is enhanced upon GTPγS binding as a result of the conformational change in SwII that tucks Trp^{211} into a hydrophobic pocket. We conducted the experiments in the background of the myrGα_i HI W258F protein, as this mutation reduced background fluorescence. We measured the time dependence of bimane quenching (Figure 5F, dashed line) and the time dependence of Trp fluorescence increases that occur upon exchange of GDP with GTPγS (Figure 5F, solid line) as described in Materials and Methods. When we compared these results, we found that the time dependence of bimane quenching essentially mirrored the time-dependent increase in Trp^{211} fluorescence, and these changes occurred at roughly the same rate (0.01 ± 0.002 s^{-1}). This indicates that the quenching of N-terminal fluorescence upon GTPγS binding is temporally linked to conformational changes in SwII that occur as a result of GDP−GTPγS exchange in each of these Gα_i proteins. Together with the observation that mutation of Trp^{211} relieves this quenching (Figure 5E), the data indicated that activation-dependent changes in the environment of the myr N terminus and Trp^{211} in SwII were due to an increased proximity between these regions in the activated protein.

DISCUSSION

This comprehensive study of myristoylated Gα_i proteins was undertaken to improve our understanding of the factors that aid in the solubility of activated myrGα proteins. The association of the myr N terminus with the surface of the protein upon GTP binding, shown as a dark dotted line in Figure 6, likely plays an important role in maintaining the solubility of myrGα proteins

dx.doi.org/10.1021/bi201472c | Biochemistry 2012, 51, 1911−1924

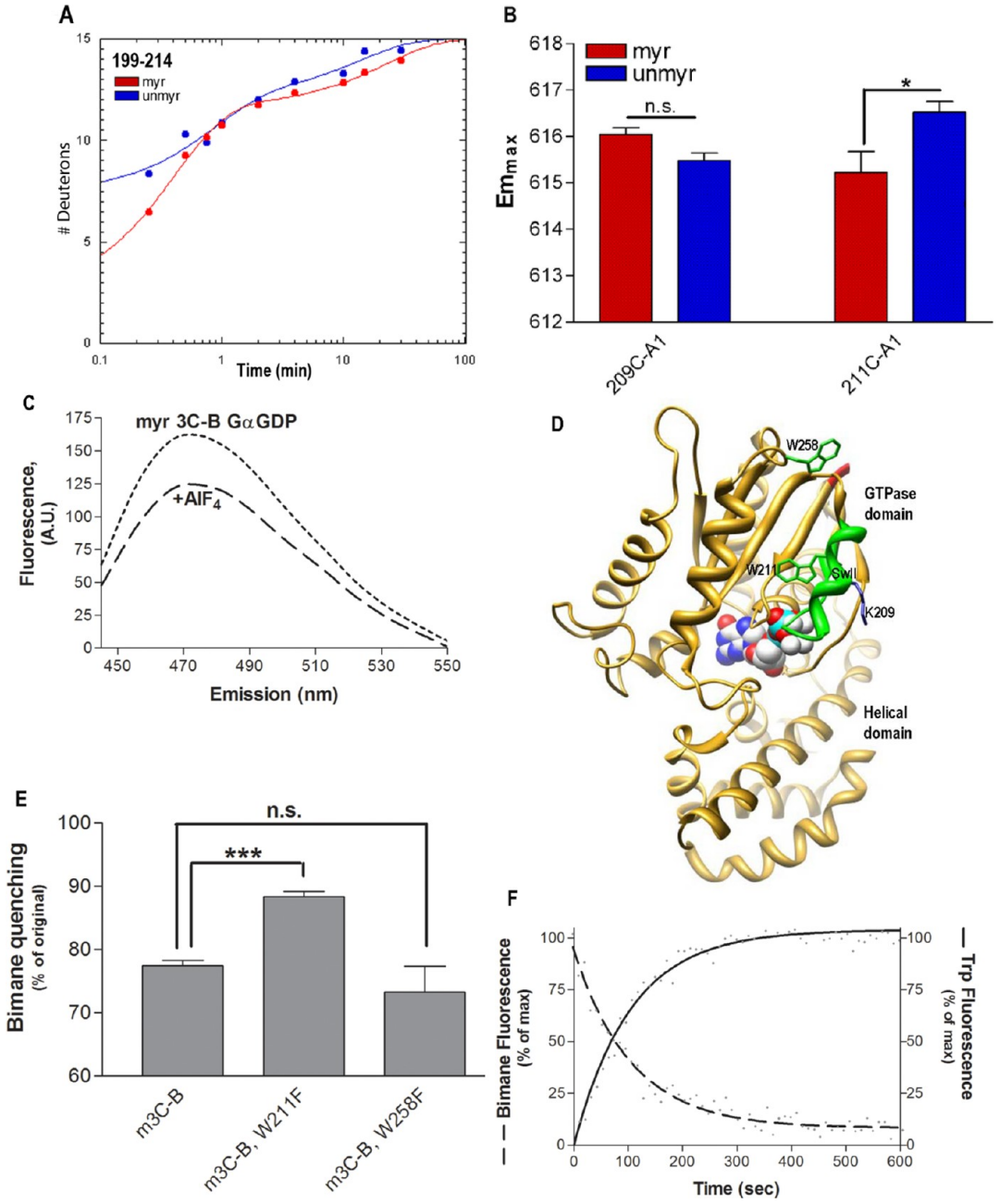

Figure 5. Environment of SwII. (A) Shown is the time dependence of H−D exchange (as described in the legend of Figure 2) for the peptide spanning residues 199−214 encompassing the SwII region. (B) em_{max} for the indicated A1-labeled $G\alpha_i$ HI proteins after AlF_4 activation was determined from excitation at 580 nm and scanning peak emission between 590 and 750 nm in a minimum of three independent experiments as described in Materials and Methods; results are means ± SEM. (C) Representative trace of bimane emission from the myr$G\alpha_i$ HI protein labeled at the third residue with bimane. Emission was scanned between 430 and 550 nm with excitation at 375 nm, before (---) and after (———) activation with AlF_4 as described in Materials and Methods. (D−F) Localization of the N terminus in myr$G\alpha_i$ proteins. (D) Location of Trp residues (side chains colored green) located within the GTPase domain of $G\alpha_i$, with the last resolved N-terminal residues colored red, and the SwII region containing W211 as a green ribbon (PDB entry 1GFI,[2] rendered with Chimera[66]). (E) Quantitation of activation-dependent quenching of bimane fluorescence performed on N-terminally labeled myr proteins containing native Trp at positions 211 and 258 (left bar), or with either Trp mutated to Phe (right two bars), as described in Materials and Methods. Results are the average of three independent experiments ± SEM. (F) The dashed line shows the time-dependent decrease in bimane fluorescence (ex/em 375/470 nm) upon addition of 10 μM GTPγS to GDP-bound myr$G\alpha_i$ HI W258F-3C-bimane, performed in triplicate, and fit to a single-exponential curve shown. The solid line shows the time-dependent increase in Trp fluorescence (ex/em 280/340) upon addition of 10 μM GTPγS to GDP-bound (unlabeled) myr$G\alpha_i$ HI W258F-3C, performed in triplicate, and fit to a single-exponential curve shown, using GraphPad Prism 4.0. Assays were performed at 18 °C as described in Materials and Methods. Data are the average of three independent experiments.

upon GTP binding through a dual disengagement of Gα from G$\beta\gamma$ and membrane fractions. Activation-dependent changes in the myr N terminus that regulates the protein's access to membranes and binding partner(s) are a defining feature of all myristoyl switching proteins, including Arf,[44] PKA,[45] HIV-Gag,[46] MARCKS,[47] c-Src,[48] recoverin,[49] and hisactophilin,[50] to

dx.doi.org/10.1021/bi201472c | *Biochemistry* 2012, 51, 1911−1924

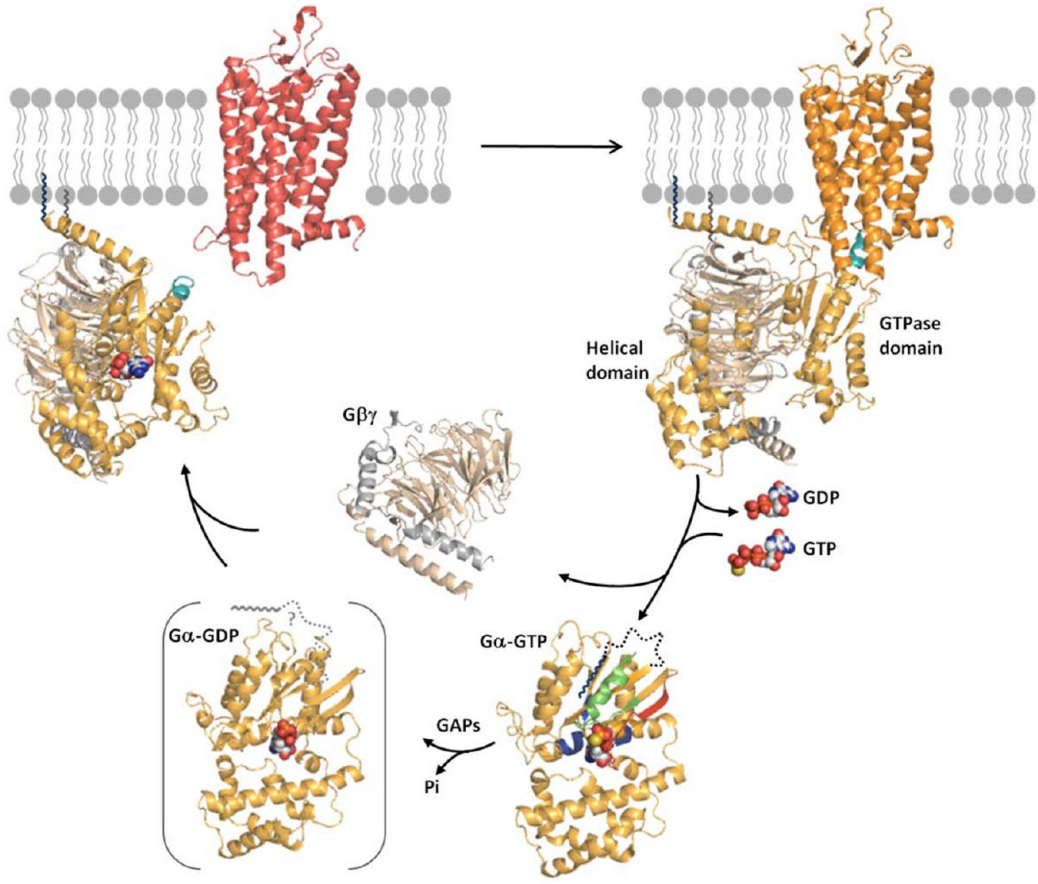

Figure 6. Model of the G protein cycle, rendered with Pymol (http://www.pymol.org). Model of the receptor-bound state taken from ref 67: inactive receptor colored red, activated receptor colored orange, C terminus of Gα colored teal, N-terminal myristate on Gα colored navy blue, and C-terminal farnesylation of Gγ colored gray. In G$\beta\gamma$, Gβ is colored brown and Gγ gray. In the GTP-bound state, N-terminal residues 2−31 are shown as a dotted line attached to myristate, with the Switch II region colored green, and other ribbons colored as in Figures 4E and 5D.

name a few, as well as Gα subunits from the G_i family of heterotrimeric G proteins.

The monomeric G protein Arf shares a number of structural and functional characteristics with heterotrimeric Gα proteins, including a homologous GTPase domain. A recent NMR structure of myr Arf[51] reveals the myristate bound in a series of overlapping orientations, indicating the intramolecular binding of the myr N terminus of Arf may be a highly dynamic process. Myristoylation of Arf also exerts allosteric effects on residues in Arf's GTPase domain, distal from the N-terminal myr site, as is the case with Gα. Allostery and protein dynamics may be general mechanisms regulating GTPases that are subject to N-terminal myristoylation such as Arf and $G\alpha_i$ family proteins, with effects that are specific to the function of each protein.

In $G\alpha_i$, the intramolecular interaction site is close to, or overlaps with, portions of the effector binding cleft, located between SwII and the α3 helix.[11,13,52−59] While the proposed binding site for the myr N terminus may appear at first glance to be at odds with cocrystal structures of unmyrGα effector proteins, this is not necessarily the case. This intramolecular binding could enhance, perturb, or have no effect on interactions with effectors, and furthermore, this could occur in an effector-specific manner. The SwII region may accommodate binding of the myr N terminus and an effector without major alterations of the binding cleft, evidenced by the RGS9−PDEγ−$G\alpha_{i/t}$ cocrystal structure, where SwII of Gα cooperatively binds both the C terminus of PDEγ and portions of RGS9.[11] Moreover, there are indications in the literature that intramolecular binding of the N terminus and effector may not be mutually exclusive, at least for the myrGα−PDEγ interaction. A cross-linking study revealed activation-dependent cross-links between residues in the myr N terminus of $G\alpha_t$ and the C terminus of PDEγ,[60] the same region of PDEγ that binds to the cleft in RGS9−PDEγ−$G\alpha_{i/t}$ complexes.[11] Taken together, the cross-linking data and crystal structure place the C terminus of PDEγ and N-terminal residues of myrGα within 10 Å of each other and the effector binding cleft, consistent with the bimane quenching we observed. This activation-dependent quenching also rules out the myr N terminus collapsing on itself as a cause for changes in the environment of specifically labeled N-terminal residues,[14,31] and the quenching is also consistent with a previous study[23] demonstrating that myr altered the solvent exposure of Trp[211] in the activated protein.

Given the fact that some Gα proteins are not myristoylated, and that unmyrGα proteins are often able to activate effectors, myristoyl switching in heterotrimeric G proteins may serve to fine-tune, rather than prevent, signaling. However, many in vitro studies comparing these effects employ N-terminally tagged recombinant $G\alpha_i$ and $G\alpha_{i/t}$ proteins. This hampers direct comparisons between myr and unmyr proteins, as does the inclusion of membrane lipids, and emphasizes the need for solution studies using untagged proteins to either confirm or rule out a direct role for myr in effector activation. For example,

dx.doi.org/10.1021/bi201472c | *Biochemistry* 2012, 51, 1911−1924

myr has been shown to enhance $G\alpha_i$ inhibition of adenylyl cyclase in experiments using membrane preparations,[61] which reflect membrane anchorage effects as well as any direct effects that might be present due to myr. Nevertheless, another study demonstrates that a myristoyl-deficient $G\alpha_{i2}$ protein remains membrane-associated but is unable to regulate adenylyl cylcase.[62] Further studies in well-defined systems are needed to determine the influence of myr on effector activation and to determine if these influences are effector-specific or more general in nature.

How do the various conformations in the N terminus relate to the G protein cycle depicted in Figure 6? Structures of unmyr heterotrimeric G proteins show the extreme amino-terminal helix of $G\alpha$ flanking a solvent-exposed face of $G\beta\gamma$ and positioned for interaction with membrane-bound receptors.[6,8,9,39] Upon receptor-mediated GTP binding, the affinity of $G\alpha$ for $G\beta\gamma$ decreases,[20,63] and the intramolecular binding sequesters the N terminus from this $G\beta\gamma$ interaction site as well as membranes. While both protein−lipid and protein−protein interactions play a role in intramolecular binding, as seen by the relatively low extent of fast H−D exchange of the N terminus in both myr- and unmyr$G\alpha$, myr may more heavily favor the bound state, driven by hydrophobic interactions and the energy cost of solvating an exposed carbon chain. The intramolecular interaction results in a predominantly soluble protein (Figure 6). The myr-dependent decrease in H−D exchange in the $\alpha4/\beta6$ loop may serve to reduce the surface area available for receptor interaction, aiding in the solubility of the myr protein. Upon hydrolysis of GTP to GDP, the N terminus of myr$G\alpha$GDP exhibits a high degree of immobility[14] (Figure 6, shown bracketed), and this conformation is also accompanied by remodeling of the SwII region.[1,2,7,23] The decreased mobility of the myr N terminus relative to the unmyr state observed in these EPR experiments indicates the N terminus of $G\alpha$ is capable of adopting distinct conformations based on the presence of the myristoyl group.[14] This is followed by $G\beta\gamma$ reassociation, leading to extrusion of the myr N terminus and subsequent burial in the membrane, where the inactive G protein remains poised for another round of activation.

This study reveals insights into forces involved in stabilization of bound nucleotide in the activated protein. In vivo, bound GTP and Mg^{2+} position a catalytically important water molecule in the phosphate binding region of $G\alpha_i$ protein, flanked by SwI and the P-loop. In mice, expression of a myristoylation-deficient $G\alpha_t$ protein results in a degree of mislocalization, and the protein that is properly localized exhibits defects in deactivation,[64] consistent with a role for myr in both localization and hydrolytic activities of the protein. The increased level of solvent exposure we detected in the P-loop as a result of myr may augment movement or positioning of this catalytic water; however, the time dependence of H−D exchange in the P-loop was unchanged by myristoylation. Dynamics of the P-loop may be stabilized by AlF_4 binding in this region or may simply be tightly regulated. The latter is suggested by a G42V mutation that increases the flexibility of the P-loop and results in a 30-fold lower k_{cat} for GTP hydrolysis versus that for wild-type $G\alpha_i$.[65] Opposite the P-loop, in the SwI region, the myr protein displays increased protein dynamics, which may serve to predispose this Switch region for conformational changes that are known to occur upon GTP hydrolysis.

The strength and duration of nucleotide binding are critically important for the function of $G\alpha$ proteins, as defects in either of these can have dramatic effects on signaling. We observed myr-dependent reductions in the level of H−D exchange at the base of the $\alpha5$ helix at nearly all time points tested. This region directly contacts the guanine ring of the bound nucleotide. Myristoylation stabilized interactions between the guanine ring and the $\alpha5$ helix, revealed by the $G\alpha_i$ D328R mutant that perturbs this interaction,[32,41] and these stabilizing effects were confirmed in wild-type $G\alpha_i$ proteins. Together, these studies suggest that myr-dependent effects on the environment and H−D exchange dynamics of residues surrounding the guanine ring serve to enhance and stabilize nucleotide binding in the activated protein.

Taken together, the subtle and not-so-subtle myr-dependent differences we uncovered reveal allosteric influences of myristoylation on activated $G\alpha$ proteins. These results are consistent with a myristoyl switching mechanism for $G\alpha$ proteins that modulates the access of these proteins to the membranes and cytosol through activation-dependent changes in the myr N terminus of $G\alpha$ subunits. Myr-dependent effects on activated $G\alpha$ proteins influenced the stability of binding of the nucleotide in activated $G\alpha$ proteins through interactions between the C-terminal $\alpha5$ helix and the guanine ring. These results provide new insights into the role of myristoylation in the spatial and temporal regulation of G protein signaling.

■ ASSOCIATED CONTENT

Ⓢ Supporting Information

Supplementary table and figures. This material is available free of charge via the Internet at http://pubs.acs.org.

■ AUTHOR INFORMATION

Corresponding Author

*Telephone: (615) 343-3533. Fax: (615) 343-1084. E-mail: heidi.hamm@vanderbilt.edu.

Author Contributions

A.M.P. and A.I.K. contributed equally to this work.

Funding

This work funded by National Institutes of Health Grants R01 EY06062 (H.E.H.) and R01 GM030910 (R.N.A.) and supported in part by Vanderbilt CTSA Grant UL1 RR024975 from the National Center for Research Resources to A.M.P. and A.I.K.

Notes

The authors declare no competing financial interest.

■ ACKNOWLEDGMENTS

We thank Guihua Liao for excellent technical assistance and Megan Nicholson for careful reading of the manuscript.

■ ABBREVIATIONS

myr, myristoylated; unmyr, unmyristoylated; ex/em, excitation/emission; BD, Bodipy; A1, Alexa; MS/MS, tandem mass spectrometry; LC, liquid chromatography; H−D, hydrogen−deuterium; HI, $G\alpha_{il}$ isoform lacking several solvent-exposed cysteines; GDP, guanosine diphosphate; GTP, guanosine triphosphate; GTPγS, guanosine 5′-*O*-(3-thiotriphosphate); BD-GTPγS, Bodipy-GTPγS; G_t, G protein of the rod outer segment, transducin; G_i, family of G proteins coupled to inhibition of adenylyl cyclase; G_s, family of G proteins coupled to activation of adenylyl cyclase; $G\alpha$, α subunits of G proteins; $G\beta\gamma$, $G\beta_1\gamma_1$ dimer of heterotrimeric G proteins that binds $G\alpha_{t/i}$ family proteins; β2-AR, β-2 adrenergic receptor; AU, arbitrary

units; amu, atomic mass unit; SEM, standard error of the mean; em_{max}, maximal emission wavelength; Arf, ADP ribosylation factor; PKA, cyclic AMP-dependent protein kinase; HIV-1 Gag, Gag protein of the human immunodeficiency virus-1; MARCKS, myristoylated alanine-rich C kinase substrate; c-Src, cellular homologue of the transforming protein of Rous sacroma virus; SDS−PAGE, sodium dodecyl sulfate−polyacrylamide gel electrophoresis; PDB, Protein Data Bank.

REFERENCES

(1) Noel, J. P., Hamm, H. E., and Sigler, P. B. (1993) The 2.2 Å crystal structure of transducin-α complexed with GTPγS. *Nature 366*, 654−663.

(2) Coleman, D. E., Berghuis, A. M., Lee, E., Linder, M. E., Gilman, A. G., and Sprang, S. R. (1994) Structures of Active Conformations of $G_{i\alpha1}$ and the Mechanism of GTP Hydrolysis. *Science 265*, 1405−1412.

(3) Mixon, M. B., Lee, E., Coleman, D. E., Berghuis, A. M., Gilman, A. G., and Sprang, S. R. (1995) Tertiary and Quaternary Structural Changes in $G_{i\alpha1}$ Induced by GTP Hydrolysis. *Science 270*, 954−960.

(4) Sondek, J., Lambright, D. G., Noel, J. P., Hamm, H. E., and Sigler, P. B. (1994) GTPase mechanism of Gproteins from the 1.7-Å crystal structure of transducin α·GDP·AlF_4^-. *Nature 372*, 276−279.

(5) Coleman, D. E., and Sprang, S. R. (1998) Crystal Structures of the G Protein $G_{i\alpha1}$ Complexed with GDP and Mg^{2+}: A Crystallographic Titration Experiment. *Biochemistry 37*, 14376−14385.

(6) Rasmussen, S. G., Devree, B. T., Zou, Y., Kruse, A. C., Chung, K. Y., Kobilka, T. S., Thian, F. S., Chae, P. S., Pardon, E., Calinski, D., Mathiesen, J. M., Shah, S. T., Lyons, J. A., Caffrey, M., Gellman, S. H., Steyaert, J., Skiniotis, G., Weis, W. I., Sunahara, R. K., and Kobilka, B. K. (2011) Crystal structure of the β_2 adrenergic receptor-Gs protein complex. *Nature 477*, 549−555.

(7) Lambright, D. G., Noel, J. P., Hamm, H. E., and Sigler, P. B. (1994) Structural determinants for activation of the α-subunit of a heterotrimeric G protein. *Nature 369*, 621−628.

(8) Lambright, D. G., Sondek, J., Bohm, A., Skiba, N. P., Hamm, H. E., and Sigler, P. B. (1996) The 2.0 Å crystal structure of a heterotrimeric G protein. *Nature 379*, 311−319.

(9) Wall, M. A., Coleman, D. E., Lee, E., Iniguez-Lluhi, J. A., Posner, B. A., Gilman, A. G., and Sprang, S. R. (1995) The Structure of the G Protein Heterotrimer $G_{i\alpha1}\beta_1\gamma_2$. *Cell 83*, 1047−1058.

(10) Tesmer, J. J., Berman, D. M., Gilman, A. G., and Sprang, S. R. (1997) Structure of RGS4 Bound to AlF_4^--activated $G_{i\alpha1}$: Stabilization of the Transition State for GTP Hydrolysis. *Cell 89*, 251−261.

(11) Slep, K. C., Kercher, M. A., He, W., Cowan, C. W., Wensel, T. G., and Sigler, P. B. (2001) Structural determinants for regulation of phosphodiesterase by a G protein at 2.0 Å. *Nature 409*, 1071−1077.

(12) Preininger, A. M., and Hamm, H. E. (2004) G protein signaling: Insights from new structures. *Sci. STKE,*, re3.

(13) Tesmer, J. J., Sunahara, R. K., Gilman, A. G., and Sprang, S. R. (1997) Crystal Structure of the Catalytic Domains of Adenylyl Cyclase in a Complex with $G_{s\alpha}$·GTPγS. *Science 278*, 1907−1916.

(14) Preininger, A. M., Van Eps, N., Yu, N. J., Medkova, M., Hubbell, W. L., and Hamm, H. E. (2003) The Myristoylated Amino Terminus of $G\alpha_{i1}$ Plays a Critical Role in the Structure and Function of $G\alpha_{i1}$ Subunits in Solution. *Biochemistry 42*, 7931−7941.

(15) Linder, M. E., Pang, I. H., Duronio, R. J., Gordon, J. I., Sternweis, P. C., and Gilman, A. G. (1991) Lipid modifications of G protein subunits. Myristoylation of Goα increases its affinity for $\beta\gamma$. *J. Biol. Chem. 266*, 4654−4659.

(16) Mumby, S. M., and Linder, M. E. (1994) Myristoylation of G-protein α subunits. *Methods Enzymol. 237*, 254−268.

(17) Chen, C. A., and Manning, D. R. (2001) Regulation of G proteins by covalent modification. *Oncogene 20*, 1643−1652.

(18) Herrmann, R., Heck, M., Henklein, P., Hofmann, K. P., and Ernst, O. P. (2006) Signal transfer from GPCRs to G proteins: Role of the Gα N-terminal region in rhodopsin-transducin coupling. *J. Biol. Chem. 281*, 30234−30241.

(19) Kisselev, O. G., and Downs, M. A. (2003) Rhodopsin Controls a Conformational Switch on the Transducin γ Subunit. *Structure 11*, 367−373.

(20) Mumby, S. M., Heukeroth, R. O., Gordon, J. I., and Gilman, A. G. (1990) G-protein α-subunit expression, myristoylation, and membrane association in COS cells. *Proc. Natl. Acad. Sci. U.S.A. 87*, 728−732.

(21) Jia, L., Linder, M. E., and Blumer, K. J. (2011) Gi/o signaling and the palmitoyltransferase DHHC2 regulate palmitate cycling and shuttling of RGS7 family-binding protein. *J. Biol. Chem. 286*, 13695−13703.

(22) Resh, M. D. (1996) Regulation of cellular signalling by fatty acid acylation and prenylation of signal transduction proteins. *Cell. Signalling 8*, 403−412.

(23) Hamm, H. E., Meier, S. M., Liao, G., and Preininger, A. M. (2009) Trp fluorescence reveals an activation-dependent cation-π interaction in the Switch II region of Gαi proteins. *Protein Sci. 18*, 2326−2335.

(24) Preininger, A. M., Parello, J., Meier, S. M., Liao, G., and Hamm, H. E. (2008) Receptor-mediated changes at the myristoylated amino terminus of $G\alpha_{il}$ proteins. *Biochemistry 47*, 10281−10293.

(25) Hoofnagle, A. N., Resing, K. A., and Ahn, N. G. (2003) Protein Analysis by Hydrogen Exchange Mass Spectrometry. *Annu. Rev. Biophys. Biomol. Struct. 32*, 1−25.

(26) Hoofnagle, A. N., Resing, K. A., and Ahn, N. G. (2004) Practical methods for deuterium exchange/mass spectrometry. *Methods Mol. Biol. 250*, 283−298.

(27) Busenlehner, L. S., and Armstrong, R. N. (2005) Insights into enzyme structure and dynamics elucidated by amide H/D exchange mass spectrometry. *Arch. Biochem. Biophys. 433*, 34−46.

(28) Asuru, A. P., and Busenlehner, L. S. (2011) Analysis of human ferrochelatase iron binding via amide hydrogen/deuterium exchange mass spectrometry. *Int. J. Mass Spectrosc. 302*, 76−84.

(29) Busenlehner, L. S., Salomonsson, L., Brzezinski, P., and Armstrong, R. N. (2006) Mapping protein dynamics in catalytic intermediates of the redox-driven proton pump cytochrome c oxidase. *Proc. Natl. Acad. Sci. U.S.A. 103*, 15398−15403.

(30) Oldham, W. M., Van Eps, N., Preininger, A. M., Hubbell, W. L., and Hamm, H. E. (2006) Mechanism of the receptor-catalyzed activation of heterotrimeric G proteins. *Nat. Struct. Mol. Biol. 13*, 772−777.

(31) Medkova, M., Preininger, A. M., Yu, N. J., Hubbell, W. L., and Hamm, H. E. (2002) Conformational Changes in the Amino-Terminal Helix of the G Protein α_{i1} Following Dissociation from G$\beta\gamma$ Subunit and Activation. *Biochemistry 41*, 9962−9972.

(32) Preininger, A., Funk, M., Meier, S., Oldham, W., Johnston, C., Adhikary, S., Kimple, A., Siderovski, D., Hamm, H., and Iverson, T. (2009) Helix dipole movement and conformational variability contribute to allosteric GDP release in Gi subunits. *Biochemistry 48*, 2630−2642.

(33) Mazzoni, M. R., and Hamm, H. E. (1993) Tryptophan207 is involved in the GTP-dependent conformational switch in the α subunit of the G protein transducin: Chymotryptic digestion patterns of the GTPγS and GDP-bound forms. *J. Protein Chem. 12*, 215−221.

(34) McEwen, D. P., Gee, K. R., Kang, H. C., and Neubig, R. R. (2002) Fluorescence approaches to study G protein mechanisms. *Methods Enzymol. 344*, 403−420.

(35) Rusconi, F., and Belghazi, M. (2002) Desktop prediction/analysis of mass spectrometric data in proteomic projects by using massXpert. *Bioinformatics 18*, 644−645.

(36) Clauser, K. R., Baker, P., and Burlingame, A. L. (1999) Role of accurate mass measurement (±10 ppm) in protein identification strategies employing MS or MS/MS and database searching. *Anal. Chem. 71*, 2871−2882.

(37) Zhang, Z., and Marshall, A. G. (1998) A universal algorithm for fast and automated charge state deconvolution of electrospray mass-to-charge ratio spectra. *J. Am. Soc. Mass Spectrom. 9*, 225−233.

(38) Van Eps, N., Oldham, W. M., Hamm, H. E., and Hubbell, W. L. (2006) Structural and dynamical changes in an α-subunit of a

heterotrimeric G protein along the activation pathway. *Proc. Natl. Acad. Sci. U.S.A. 103*, 16194−16199.
(39) Hu, J., Wang, Y., Zhang, X., Lloyd, J. R., Li, J. H., Karpiak, J., Costanzi, S., and Wess, J. (2010) Structural basis of G protein-coupled receptor-G protein interactions. *Nat. Chem. Biol. 6*, 541−548.
(40) Oldham, W. M., and Hamm, H. E. (2008) Heterotrimeric G protein activation by G-protein-coupled receptors. *Nat. Rev. Mol. Cell Biol. 9*, 60−71.
(41) Kapoor, N., Menon, S. T., Chauhan, R., Sachdev, P., and Sakmar, T. P. (2009) Structural evidence for a sequential release mechanism for activation of heterotrimeric G proteins. *J. Mol. Biol. 393*, 882−897.
(42) Faurobert, E., Otto-Bruc, A., Chardin, P., and Chabre, M. (1993) Tryptophan W207 in transducin Tα is the fluorescence sensor of the G protein activation switch and is involved in the effector binding. *EMBO J. 12*, 4191−4198.
(43) Mansoor, S. E., McHaourab, H. S., and Farrens, D. L. (2002) Mapping proximity within proteins using fluorescence spectroscopy. A study of T4 lysozyme showing that tryptophan residues quench bimane fluorescence. *Biochemistry 41*, 2475−2484.
(44) Goldberg, J. (1998) Structural Basis for Activation of ARF GTPase: Mechanisms of Guanine Nucleotide Exchange and GTP-Myristoyl Switching. *Cell 95*, 237−248.
(45) Gangal, M., Clifford, T., Deich, J., Cheng, X., Taylor, S. S., and Johnson, D. A. (1999) Mobilization of the A-kinase N-myristate through an isoform-specific intermolecular switch. *Proc. Natl. Acad. Sci. U.S.A. 96*, 12394−12399.
(46) Tang, C., Loeliger, E., Luncsford, P., Kinde, I., Beckett, D., and Summers, M. F. (2004) Entropic switch regulates myristate exposure in the HIV-1 matrix protein. *Proc. Natl. Acad. Sci. U.S.A. 101*, 517−522.
(47) Seykora, J. T., Myat, M. M., Allen, L. A., Ravetch, J. V., and Aderem, A. (1996) Molecular determinants of the myristoyl-electrostatic switch of MARCKS. *J. Biol. Chem. 271*, 18797−18802.
(48) Patwardhan, P., and Resh, M. D. (2010) Myristoylation and membrane binding regulate c-Src stability and kinase activity. *Mol. Cell. Biol. 30*, 4094−4107.
(49) Ames, J. B., Tanaka, T., Stryer, L., and Ikura, M. (1994) Secondary structure of myristoylated recoverin determined by three-dimensional heteronuclear NMR: Implications for the calcium-myristoyl switch. *Biochemistry 33*, 10743−10753.
(50) Hanakam, F., Gerisch, G., Lotz, S., Alt, T., and Seelig, A. (1996) Binding of hisactophilin I and II to lipid membranes is controlled by a pH-dependent myristoyl-histidine switch. *Biochemistry 35*, 11036−11044.
(51) Liu, Y., Kahn, R. A., and Prestegard, J. H. (2010) Dynamic structure of membrane-anchored Arf*GTP. *Nat. Struct. Mol. Biol. 17*, 876−881.
(52) Yan, S. Z., Huang, Z. H., Rao, V. D., Hurley, J. H., and Tang, W. J. (1997) Three discrete regions of mammalian adenylyl cyclase form a site for Gsα activation. *J. Biol. Chem. 272*, 18849−18854.
(53) Tesmer, J. J., Sunahara, R. K., Johnson, R. A., Gosselin, G., Gilman, A. G., and Sprang, S. R. (1999) Two-Metal-Ion Catalysis in Adenylyl Cyclase. *Science 285*, 756−760.
(54) Chen, Z., Singer, W. D., Sternweis, P. C., and Sprang, S. R. (2005) Structure of the p115RhoGEF rgRGS domain-Gα13/i1 chimera complex suggests convergent evolution of a GTPase activator. *Nat. Struct. Mol. Biol. 12*, 191−197.
(55) Tesmer, V. M., Kawano, T., Shankaranarayanan, A., Kozasa, T., and Tesmer, J. J. (2005) Snapshot of Activated G Proteins at the Membrane: The $G\alpha_q$-GRK2-Gβγ Complex. *Science 310*, 1686−1690.
(56) Skiba, N. P., Bae, H., and Hamm, H. E. (1996) Mapping of Effector binding Sites of Transducin α-Subunit Using $G\alpha_t/G\alpha_{i1}$ Chimeras. *J. Biol. Chem. 271*, 413−424.
(57) Venkatakrishnan, G., and Exton, J. H. (1996) Identification of determinants in the α-subunit of Gq required for phospholipase C activation. *J. Biol. Chem. 271*, 5066−5072.
(58) Artemyev, N. O., Mills, J. S., Thornburg, K. R., Knapp, D. R., Schey, K. L., and Hamm, H. E. (1993) A site on transducin α-subunit of interaction with the polycationic region of cGMP phosphodiesterase inhibitory subunit. *J. Biol. Chem. 268*, 23611−23615.
(59) Artemyev, N. O., Natochin, M., Busman, M., Schey, K. L., and Hamm, H. E. (1996) Mechanism of photoreceptor cGMP phosphodiesterase inhibition by its γ-subunits. *Proc. Natl. Acad. Sci. U.S.A. 93*, 5407−5412.
(60) Grant, J. E., Guo, L. W., Vestling, M. M., Martemyanov, K. A., Arshavsky, V. Y., and Ruoho, A. E. (2006) The N terminus of GTPγS-activated transducin α-subunit interacts with the C terminus of the cGMP phosphodiesterase γ-subunit. *J. Biol. Chem. 281*, 6194−6202.
(61) Taussig, R., Iniguez-Lluhi, J. A., and Gilman, A. G. (1993) Inhibition of Adenylyl Cyclase by $G_{i\alpha}$. *Science 261*, 218−221.
(62) Gallego, C., Gupta, S. K., Winitz, S., Eisfelder, B. J., and Johnson, G. L. (1992) Myristoylation of the $G\alpha_{i2}$ polypeptide, a G protein α subunit, is required for its signaling and transformation functions. *Proc. Natl. Acad. Sci. U.S.A. 89*, 9695−9699.
(63) Linder, M. E., Pang, I. H., Duronio, R. J., Gordon, J. I., Sternweis, P. C., and Gilman, A. G. (1991) Lipid Modifications of G Protein Subunits. Myristoylation of $G_{o\alpha}$ Increases its Affinity for βγ. *J. Biol. Chem. 266*, 4654−4659.
(64) Kerov, V., Rubin, W. W., Natochin, M., Melling, N. A., Burns, M. E., and Artemyev, N. O. (2007) N-terminal fatty acylation of transducin profoundly influences its localization and the kinetics of photoresponse in rods. *J. Neurosci. 27*, 10270−10277.
(65) Raw, A. S., Coleman, D. E., Gilman, A. G., and Sprang, S. R. (1997) Structural and Biochemical Characterization of the GTPγS-, GDP·Pi-, and GDP-bound Forms of a GTPase-Deficient $Gly^{42} \rightarrow Val$ mutant of $G_{i\alpha1}$. *Biochemistry 36*, 15660−15669.
(66) Pettersen, E. F., Goddard, T. D., Huang, C. C., Couch, G. S., Greenblatt, D. M., Meng, E. C., and Ferrin, T. E. (2004) UCSF Chimera: A visualization system for exploratory research and analysis. *J. Comput. Chem. 25*, 1605−1612.
(67) Van Eps, N., Preininger, A. M., Alexander, N., Kaya, A. I., Meier, S., Meiler, J., Hamm, H. E., and Hubbell, W. L. (2011) Interaction of a G protein with an activated receptor opens the interdomain interface in the α subunit. *Proc. Natl. Acad. Sci. U.S.A. 108*, 9420−9424.